

Dynamic Mobile-Former: Strengthening Dynamic Convolution with Attention and Residual Connection in Kernel Space

Seokju Yun Youngmin Ro

Machine Intelligence Laboratory, University of Seoul, Korea

{wsz871, youngmin.ro}@uos.ac.kr

Abstract

We introduce *Dynamic Mobile-Former(DMF)*, maximizes the capabilities of dynamic convolution by harmonizing it with efficient operators. Our *Dynamic Mobile-Former* effectively utilizes the advantages of *Dynamic MobileNet* (*MobileNet* equipped with dynamic convolution) using global information from light-weight attention. A *Transformer* in *Dynamic Mobile-Former* only requires a few randomly initialized tokens to calculate global features, making it computationally efficient. And a bridge between *Dynamic MobileNet* and *Transformer* allows for bidirectional integration of local and global features. We also simplify the optimization process of vanilla dynamic convolution by splitting the convolution kernel into an input-agnostic kernel and an input-dependent kernel. This allows for optimization in a wider kernel space, resulting in enhanced capacity. By integrating lightweight attention and enhanced dynamic convolution, our *Dynamic Mobile-Former* achieves not only high efficiency, but also strong performance. We benchmark the *Dynamic Mobile-Former* on a series of vision tasks, and showcase that it achieves impressive performance on image classification, COCO detection, and instance segmentation. For example, our *DMF* hits the top-1 accuracy of 79.4% on *ImageNet-1K*, much higher than *PVT-Tiny* by 4.3% with only 1/4 FLOPs. Additionally, our proposed *DMF-S* model performed well on challenging vision datasets such as COCO, achieving a 39.0% mAP, which is 1% higher than that of the *Mobile-Former 508M* model, despite using 3 GFLOPs less computations. Code and models are available at <https://github.com/ysj9909/DMF>

1. Introduction

Recently, vision transformer(ViT) [1, 2] demonstrates the advantage of global processing and excellent capabilities with scalability over convolutional neural networks (CNNs). However, since ViT has a time complexity that

scales quadratically with the sequence length, its computational efficiency decreases when working with longer sequences, making it more challenging to train and deploy ViT models in scenarios with limited computational resources. If we reduce the computational cost to under 500M FLOPs, *MobileNet* [3–5] and other similar-sized lightweight CNNs [6–8] still outperform ViT variants in terms of efficiency, thanks to their ability to perform local processing using techniques such as depth-wise separable convolution [4] and group convolution with channel shuffle [6, 7].

Along with great advances in efficient CNN architecture design, dynamic convolution [9, 10] has recently gained popularity for the implementation of lightweight networks due to its ability to achieve significant performance gains with negligible computational cost. This has led to its adoption for multiple vision tasks [10–15]. Moreover, as many computer vision applications are not constrained by the number of parameters, but instead have strict latency requirements for inference, such as real-time object detection and tracking for autonomous driving, the potential of using dynamic convolution in these scenarios is increasing.

The basic idea of dynamic convolution is to dynamically aggregate multiple convolution kernels into a convolution weight matrix, using an input-dependent attention mechanism.

$$\mathbf{W}_{dynamic}(x) = \sum_{k=1}^K \pi_k(x) \mathbf{W}_{static}^k \quad s.t. \quad 0 \leq \pi_k(x) \leq 1, \quad (1)$$

where K static convolution kernels \mathbf{W}_{static}^k are weighted summed using attention scores $\pi_k(x)$.

Dynamic convolution has two limitations: 1) The input to a kernel attention module may have limited representational power, which can restrict the ability of the attention mechanism to calculate relevant filters effectively. 2) a joint optimization of attention scores and static kernels can be challenging. In this work, we propose our dynamic residual group convolution that can efficiently compute input-specific local features while addresses the limitations mentioned above.

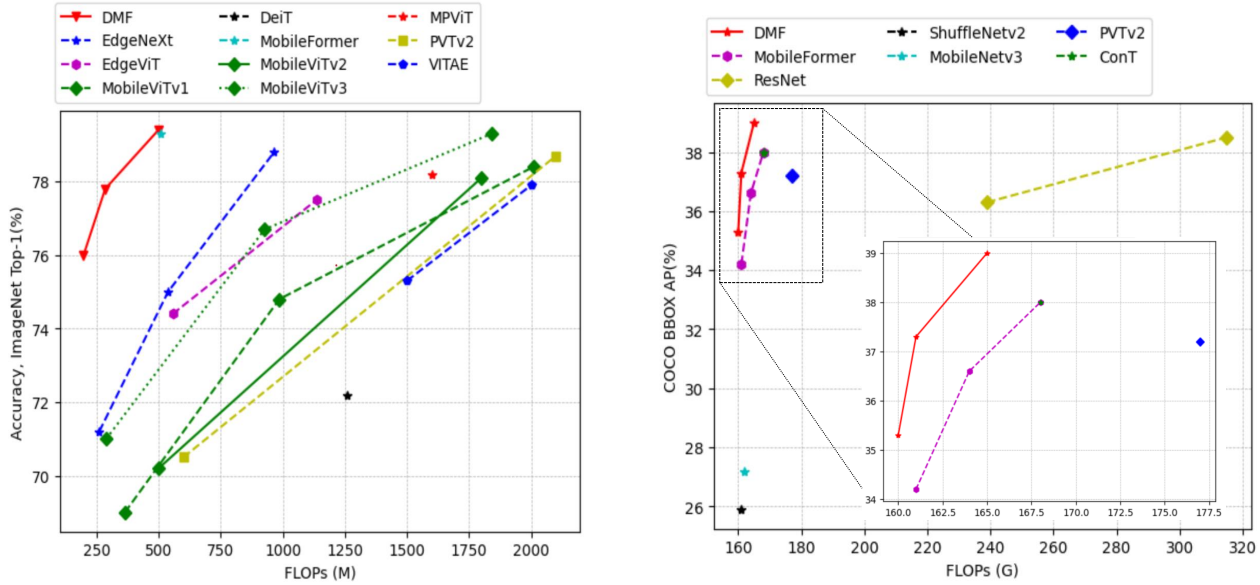


Figure 1. **Performance comparison between DMF and other methods.** Left: Top-1 accuracy on ImageNet-1K [16]. Right: Object detection results on COCO val2017 [17] of various backbones using RetinaNet [18] framework, all numbers are for single-scale training, 12 epochs (1×) training schedule. Best viewed in color.

[9, 10] uses the global average pooled features as inputs to the kernel attention module to generate attention scores. However, spatially squeezed features have limited representational power, because all features at each location are merged with the same weight. To solve this limitation, our Dynamic Mobile-Former utilizes global salient features, which are calculated using light-weight attention, as input to the kernel attention module. This allows appropriate kernels to be selected for each input.

And [9] proposed the use of a sigmoid layer to generate attention scores, leading to a significantly large space for the convolution kernel that makes the learning of attention scores difficult. [10] replaced the sigmoid layer with a softmax function to compress the kernel space, thereby facilitating learning of the attention module. However, the model capacity is reduced as the kernel space is limited. To solve this problem, we separate the existing convolution kernel into an input-agnostic kernel and an input-dependent kernel to ease learning of the kernel attention module. In addition to our method, we use sigmoid activation to achieve better performance than [9, 10]. Its effectiveness has been verified by experimental results in section 4.3. We also propose a more efficient module by combining the above techniques with group convolution (see section 3.3).

Our DMF model achieves superior performance in terms of both accuracy and FLOPs, as demonstrated through extensive experiments on ImageNet and other downstream tasks. Our method shows the favorable tradeoff between accuracy and FLOPs (see Fig. 1). For example, DMF-S achieves 79.4% top-1 accuracy on ImageNet, which is higher than that of the MobileFormer-508M [19] (current

state-of-the-art) with less computations. DMF-S also hits 0.5% higher performance in COCO detection compared to ResNet101 [20], while utilizing almost half the computations required by ResNet101 (315G → 165G).

2. Related Work

Efficient CNNs: MobileNet [3–5] uses depthwise separable convolution to decompose a standard $k \times k$ convolution into a depthwise convolution and a pointwise convolution. ShuffleNet [6, 7] combines group convolution and channel shuffle to improve the efficiency of the network. EfficientNet [8, 21] proposes a compound scaling method that scales up the depth, width, and resolution of the network in a principled manner. Other efficient operators include cheap linear transformations in GhostNet [22], mixing up multiple kernel sizes [23], and using additions to trade multiplications in AdderNet [24]. Our Dynamic Mobile-Former effectively combines the efficient operators such as depthwise separable convolution, group convolution presented mentioned above.

Vision Transformers and efficient variants: The pioneering work ViT [1] directly applied the transformer [25] to classification with image patches as input. Since then, there have been numerous attempts [2, 26–35] to apply transformer in computer vision tasks. Furthermore, research aimed at harmonizing strengths of ViT and CNN models [26, 31, 36–42] has gained popularity in the computer vision community. [26, 31, 38] leverage a convolutional projection into a vanilla attention [1, 25] module. There are studies that utilize both attention and convolutional blocks either sequentially [36, 40] or in parallel [19, 37, 41, 42].

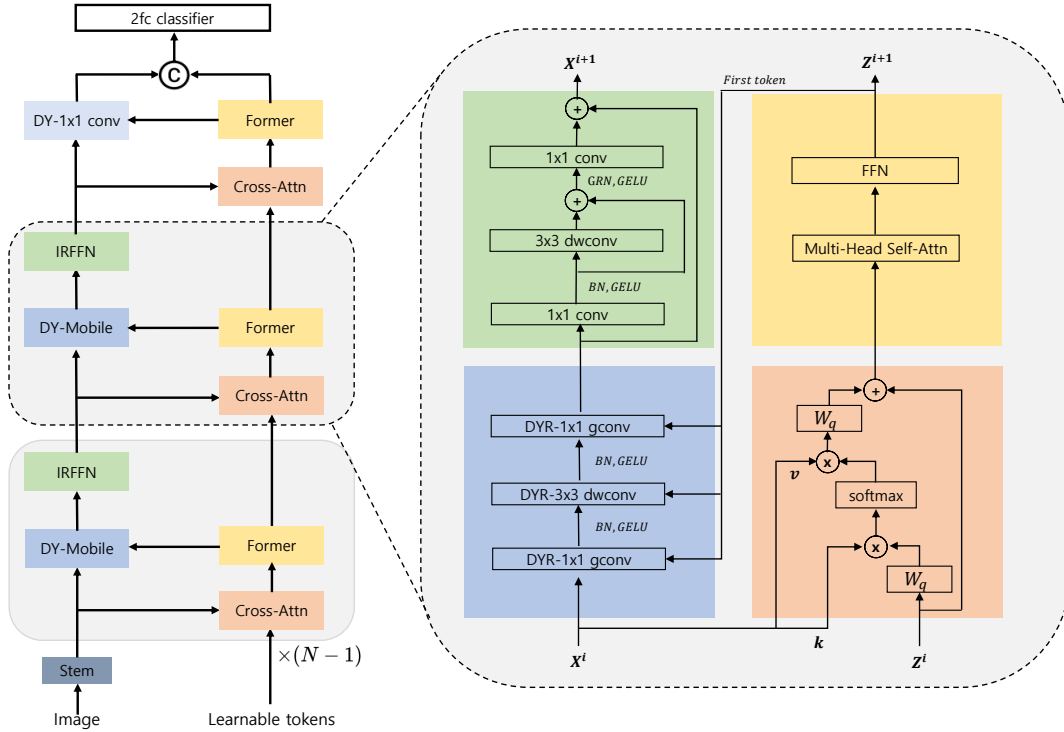


Figure 2. **The overall architecture of Dynamic Mobile-Former(DMF) and details of DMF block.** Following [19], Dynamic Mobile-Former adopts parallel design for processing both local and global features. Each layer includes a Dynamic Mobile block, a cross attention block, a Former block, and a Inverted Residual FFN. Also DYN-gconv and DYN-dwconv in Dynamic Mobile block means dynamic residual group convolution, dynamic residual depth-wise convolution respectively. Best viewed in color.

Different from the above ViT variants, there is another line of works [19, 43] that use cross-attention with very few learnable tokens. Our Dynamic Mobile-Former also uses cross-attention with very few learnable tokens for calculating global salient features. Our Dynamic Mobile-Former endows Dynamic Convolution [9, 10] to convey global information to local features, in contrast to [19] which utilizes cross-attention.

Dynamic Neural Networks: Dynamic networks increase their representation power by adjusting their parameters or activation functions [44] based on the input. [45, 46] recalibrates channel information by squeezing global context. Dynamic convolution [9, 10] aggregates multiple kernels based on input dependent attention. DCD [47] proposes a dynamic convolution decomposition method which can get more compact yet competitive models to handle limitations of the dynamic convolution. ODConv [48] introduces a dynamic convolution approach that is not only computationally efficient, but also parametrically efficient. Instead, in this paper we also aim to address the limitations of dynamic convolution in different manner, see the Introduction and Method sections for details.

3. Dynamic Mobile-Former

3.1. Overall Architecture

As shown in Fig. 2, Dynamic Mobile-Former(DMF) combines the MobileNet [4] and Transformer [1] using dynamic convolution and lightweight cross attention. DY-Mobile (refers to Dynamic Mobile block) extracts local features input-dependently from an input image, while Former and Cross-Attn (refer to Transformer block and cross attention layer, respectively) extract global features using learnable tokens. Unlike ViT, which projects local image patches linearly, Former and Cross-Attn use significantly fewer parameters (e.g. 6 or fewer tokens) resulting in reduced computational cost. As mentioned in [36], ViTs and CNNs are complementary, and it is important to combine features of attention and convolution appropriately. To achieve this goal, different approaches have been proposed such as adding attention layers at the end of each stage as in [36], configuring two layers in parallel and element-wise adding their outputs as in [42], and utilizing cross-attention layers as in [19]. Following [19], our DMF uses cross attention layer to fuse local features to global tokens. However, to fuse global tokens into local features, we input the global token into the kernel attention module in dynamic convolu-

tion [9, 10].

To improve model efficiency, we use group convolutions on 1x1 layers, which reduces computational costs by ensuring each convolution operates on its corresponding input channel group. However, when multiple group convolutions are stacked together, a side effect can occur where the outputs from a particular channel are derived from only a small fraction of input channels. To enable feature communication between different groups of channels, we apply Inverted Residual Feed-Forward Network (IRFFN) [38] after the DY-Mobile. Fully-connected layers in IRFFN can solve the above problem by connecting all channels of groups that are separated from each other. The DMF block is able to capture local dependencies by generating input-specific kernel using global information.

3.2. DMF Block

The proposed DMF block consists of a Dynamic Mobile block (DY-Mobile), a Former block with cross attention layer, and an Inverted Residual Feed-Forward Network (IRFFN), as illustrated in Fig. 2 right. DMF block has two inputs. 1) Local feature map $\mathbf{X}^i \in \mathbb{R}^{N \times C}$ with C channels and sequence length $N = H \times W$ (the resolution of the input of current block), and 2) global tokens $\mathbf{Z}^i \in \mathbb{R}^{M \times d}$, where M and d are the number and dimension of tokens, respectively. Note that M and d are consistent across all blocks. DMF block outputs the updated local feature map \mathbf{X}^{i+1} and global tokens \mathbf{Z}^{i+1} , which are used as input for the subsequent block. We will describe these Four parts in the following.

3.3. DY-Mobile

DY-Mobile is built based on the inverted bottleneck in [4] with three modifications. Firstly, we substitute all vanilla convolutions with our dynamic residual convolutions. The dynamic residual convolution kernel consists of two parts: an input-agnostic kernel and a dynamic kernel calculated as Eq. 1. specifically, adding the input-agnostic kernel to vanilla dynamic kernel leads to

$$\mathbf{W}_{dy-res}(x) = \mathbf{W}_{dynamic}(x) + \mathbf{W}_{input-agnostic}$$

$$\text{where } \mathbf{W}_{dynamic}(x) = \sum_{k=1}^K \pi_k(x) \mathbf{W}_{static}^k, \quad 0 \leq \pi_k(x) \leq 1, \quad (2)$$

Where \mathbf{W}_{static} and $\mathbf{W}_{input-agnostic}$ are static but \mathbf{W}_{static} is initialized to zero while $\mathbf{W}_{input-agnostic}$ is initialized randomly. Fig. 3 provides a schematic visualization of dynamic residual convolution layer. specifically, to compute attention scores, we use sigmoid activation function. And following [10], we adopt a temperature annealing strategy in the early training process to suppress the near zero output of the sigmoid function. By doing so, all convolution kernels are optimized simultaneously in early training epochs.

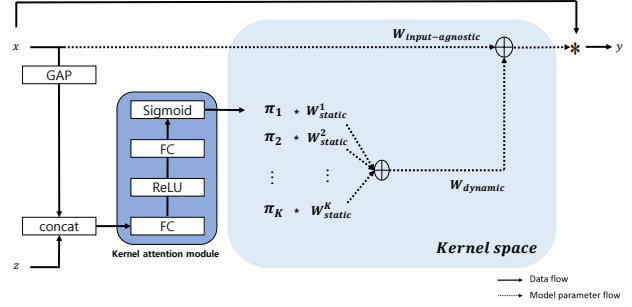


Figure 3. **A Dynamic Residual Convolution layer.** Firstly, the global average pooled features of the input and the first global token are concatenated. These concatenated features are then passed through a kernel attention module to generate attention scores (π) and obtain dynamic convolution weights using Eq. 1. Finally, a dynamic residual kernel is obtained by adding the obtained dynamic kernel and the input-agnostic kernel as described in Eq. 2. And \mathbf{W}_{static} are zero initialized according to the concept of residual connection, but $\mathbf{W}_{input-agnostic}$ is initialized randomly.

Secondly, we use group convolution for point-wise convolution. Since a high expansion ratio (3 - 6) is used in the block [4], efficiency can be greatly increased by using group convolution. Lastly, we replace ReLU with GELU [49] as the activation function, following [50]. Note that the kernel size of depth-wise convolution is 3×3 for all layers. DY-Mobile consumes computations of $O(NC^2)$. Along with IRFFN (specified in sec 3.5), it accounts for the majority of the computational complexity.

3.4. Former with Cross Attention

The light-weight cross attention from local feature map \mathbf{X} to global tokens \mathbf{Z} is computed as:

$$\text{CrossAttn} = \text{Concat}(\text{head}_1, \dots, \text{head}_N) \mathbf{W}^O, \quad (3)$$

$$\text{head}_i = \text{Attention}(\mathbf{Z}_i \mathbf{W}_i^Q, \mathbf{X}_i, \mathbf{X}_i), \quad (4)$$

$$\text{Attention}(\mathbf{q}, \mathbf{k}, \mathbf{v}) = \text{Softmax}(\mathbf{q} \mathbf{k}^T / \sqrt{d_{head}}) \mathbf{v}, \quad (5)$$

where $\text{Concat}(\cdot)$ is the concatenation operation. $\mathbf{W}_i^Q \in \mathbb{R}^{d \times d_{head}}$ and $\mathbf{W}^O \in \mathbb{R}^{d \times d}$ are linear projection weights. N is the head number of the attention layer. Therefore, the dimension of each head d_{head} is equal to $\frac{d}{N}$. To reduce computational requirements from high resolution feature map \mathbf{X} , we eliminate the projections ($\mathbf{W}^K, \mathbf{W}^V$). Through these formulas, the tokens Z are able to learn global priors. The subsequent Former sub-block is a standard Transformer [25] block including a multi-head self attention and a feed-forward network (FFN). An expansion ratio of 2 is utilized for FFN. The global features, obtained as described above, is fed into the dynamic residual convolutions. When processing an input feature map of size

stage (output size)	DMF - S			DMF - XS			DMF - XXS		
	operator	#exp	#out	operator	#exp	#out	operator	#exp	#out
Tokens (# heads)	6 × 192 (8)			6 × 192 (8)			6 × 192 (8)		
Stem (112 × 112)	vanilla 3×3conv	-	24	vanilla 3×3conv	-	16	vanilla 3×3conv	-	12
1 (112 × 112)	bneck-lite	48	24	bneck-lite	32	18	bneck-lite	24	12
Downsampling	3×3 dwconv	-	24	dwconv 3×3	-	18	3×3 dwconv	-	12
2 (56 × 56)	DMF block(2,4,2.7)	144	40	DMF block(2,3,2)	108	30	DMF block(2,2,3)	72	20
2 (56 × 56)	DMF block(2,4,2.7)	120	40	DMF block(2,3,2)	90	30	DMF block(2,2,3)	60	20
Downsampling	3×3 dwconv	-	40	3×3 dwconv	-	30	3×3 dwconv	-	20
3 (28 × 28)	DMF block(2,4,2.7)	240	72	DMF block(2,3,2)	180	54	DMF block(2,2,3)	120	36
3 (28 × 28)	DMF block(2,4,2.7)	216	72	DMF block(2,3,2)	162	54	DMF block(2,2,3)	108	36
Downsampling	3×3 dwconv	-	72	3×3 dwconv	-	54	3×3 dwconv	-	36
4 (14 × 14)	DMF block(2,4,2.7)	432	128	DMF block(2,3,2)	324	96	DMF block(2,2,3)	216	64
4 (14 × 14)	DMF block(4,4,2.7)	512	128	DMF block(3,3,2)	384	96	DMF block(2,2,3)	256	64
4 (14 × 14)	DMF block(4,4,2.7)	768	176	DMF block(3,3,2)	576	132	DMF block(2,2,3)	384	88
4 (14 × 14)	DMF block(4,4,2.7)	1056	176	DMF block(4,3,2)	792	132	DMF block(4,2,3)	528	88
Downsampling	3×3 dwconv	-	176	3×3 dwconv	-	132	3×3 dwconv	-	88
5 (7 × 7)	DMF block(4,4,2.7)	1056	240	DMF block(4,3,2)	792	180	DMF block(4,2,3)	528	120
5 (7 × 7)	DMF block(8,4,2.7)	1440	240	DMF block(6,3,2)	1080	180	DMF block(4,2,3)	720	120
5 (7 × 7)	DMF block(8,4,2.7)	1440	240	DMF block(6,3,2)	1080	180	DMF block(4,2,3)	720	120
5 (7 × 7)	DYR - 1×1conv	-	1440	DYR - 1×1conv	-	1152	DYR - 1×1conv	-	960
pool & concat	-	-	1632	-	-	1344	-	-	1152
FC1	-	-	1920	-	-	1920	-	-	1600
FC2	-	-	1000	-	-	1000	-	-	1000
# FLOPs	499M			285M			198M		

Table 1. **Dynamic Mobile-Former Architectures.** The "bneck-lite" refers to the lite bottleneck block [51]. "DYR - 1×1conv" denotes our dynamic residual point-wise convolution. We employ depth-wise convolution with stride 2 to handle the spatial downsampling. All dynamic residual convolutions used in models use 8 static kernels. "DMF block(H, G, R)" denotes Dynamic Mobile-Former block with H heads for the cross attention layer, G groups for the point-wise convolution in DY-Mobile, and R expansion ratio for the IRFFN, respectively.

$N \times C$ along with M global tokens of dimension d , Former model with cross-attention has a computational complexity of $O(M^2d + Md^2 + MNC + MdC)$.

3.5. IRFFN

The IRFFN sub-block differs slightly from the inverted residual FFN in [38] by replacing Batch Normalization [52] after shortcut connection with Global Response Normalization (GRN) [53]. Specifically, the first layer expands the dimension by a factor of a certain number, and the second layer reduces the dimension by the same ratio. Between these two layers, the depth-wise convolution with shortcut connection is used:

$$\text{IRFFN}(\mathbf{X}) = 1\times 1\text{Conv}(\text{SC}(1\times 1\text{Conv}(\mathbf{X}))), \quad (6)$$

$$\text{SC}(\mathbf{X}) = 3\times 3\text{DWConv}(\mathbf{X}) + \mathbf{X}, \quad (7)$$

where the activation (GELU [49]), GRN is omitted. We also include the batch normalization [52] after two 1×1 convolutions. This alteration facilitates communication between features that were calculated independently in each channel group of previous DY-Mobile. By using GRN [53], various features can be calculated in different groups in subsequent DY-Mobile. This sub-block has the same computa-

tional costs as DY-Mobile ($O(NC^2)$).

3.6. Model Specification

Table 1 shows the detailed architectures at different computational complexities (i.e. 499M - 198M FLOPs). Dynamic Mobile-Former (DMF) has three models with different configurations based on the number of groups in DY-Mobile. While they share similar model designs in terms of having the same number of channels per group, they differ in the number of groups and expansion ratio in IRFFN. As an illustration, DMF with 499M FLOPs for image size 224×224 , which stacks 11 DMF blocks. All blocks contain six global tokens with a dimension of 192, following [19]. It begins with a 3×3 convolution as stem and a lite bottleneck block [51] in stage 1. The bottleneck block expands and then squeezes the number of channels by stacking a 3×3 depth-wise and point-wise convolution. For downsampling across multiple blocks, a 3×3 depth-wise convolution with stride of 2 is used. To compute head input, we concatenate global average pooled local features with first global token. These features are then passed through two fully-connected layers with hard-swish [5] in between.

DMF generates four hierarchical feature maps with vary-

Model	#Pub	Reso.	#Params	FLOPs	Top-1
EdgeViT-XXS [54]	ECCV'22	256 ²	4.1M	557M	74.4
EdgeNeXt-XS [55]	ECCVW'22	256 ²	2.3M	538M	75.0
MobileNetV3 1.0x [5]	ICCV'19	224 ²	5.4M	217M	75.2
MobileNetV2 1.0x+ODConv 4x [48]	ICLR'22	224 ²	11.5M	327M	75.4
DMF-XXS	-	224 ²	15.1M	198M	76.0
ConT-S [56]	arXiv'21	224 ²	10.1M	1.5G	76.5
EfficientNet-B0 [8]	ICML'19	224 ²	5.3M	390M	77.1
Swin-1G [29] [†]	ICCV'21	224 ²	7.3M	1.0G	77.3
EfficientViT [57]	arXiv'22	192 ²	7.9M	304M	77.7
DMF-XS	-	224 ²	19.8M	285M	77.8
PVT-T [30]	ICCV'21	224 ²	13.2M	1.9G	75.1
EdgeViT-XS [54]	ECCV'22	256 ²	6.7M	2.0G	77.5
MPViT-T [58]	CVPR'22	224 ²	5.8M	1.6G	78.2
MobileViT-S [59]	ICLR'22	256 ²	5.6M	2.0G	78.4
EfficientNetV2-B0 [60]	ICML'21	224 ²	7.4M	700M	78.7
EdgeNeXt-S [55]	ECCVW'22	224 ²	5.6M	965M	78.8
BoT-S1-50 [61]	CVPR'21	224 ²	20.8M	4.3G	79.1
CMT-T [38]	CVPR'22	160 ²	9.5M	600M	79.1
Swin-2G [29] [†]	ICCV'21	224 ²	12.8M	2.0G	79.2
MobileFormer-508M [19]	CVPR'22	224 ²	14.0M	508M	79.3
DMF-S	-	224 ²	25.1M	499M	79.4

Table 2. Comparison on ImageNet-1k benchmark. light-weight CNNs, ViT variants, and hybrid models with similar accuracy are grouped together for comparison. The proposed DMFs consistently outperform other models with less computational budget. [†] means the results are from [19].

ing resolutions, similar to [4, 8, 20, 30, 38]. These feature maps have strides of 4, 8, 16, and 32 with respect to the input image, enabling DMF to obtain multi-scale representations. This makes DMF well-suited for downstream tasks such as object detection and instance segmentation, as it can capture both fine and coarse details of an object at different scales.

4. Experiments

In this section, we evaluate the proposed Dynamic Mobile-Former on ImageNet-1K classification [16], COCO object detection [17], and instance segmentation, by comparing it with representative ViTs, CNNs and their hybrid models. Ablation analysis is also conducted to showcase the contribution of each novelty in our method. Our implementation is based on PyTorch library [62] and Timm codebase [63].

4.1. ImageNet Classification

Implementation Details. ImageNet [16] provides approximately 1.28M training and 50K validation images for 1000 categories. We train our Dynamic Mobile-Former(DMF) models at an input resolution of 224x224 with a batch size of 1024. All models are trained from scratch using AdamW [64] optimizer for 470 epochs. We use cosine learning rate schedule [65] with linear warmup for 20 epochs. Data augmentation includes Random Erasing [66], Horizontal Flip, Random Resized Crop(RRC), and RandAugmentation [67]. Further we use multi-scale sampler [59] during training. For regularization, we use weight

AFKA	RCKS	#Params	FLOPs	Top-1
✗	✗	10.0M	194.0M	73.5
✓	✗	12.6M	196.6M	73.6 (+ 0.1)
✗	✓	12.4M	195.9M	74.2 (+ 0.7)
✓	✓	15.1M	198.0M	74.6 (+ 1.1)

Table 3. **Ablation of AFKA and RCKS.** Here, DMF-XXS is used and all models are trained on ImageNet dataset for 250 epochs. "AFKA" and "RCKS" mean Attention Features for Kernal Attention module, Residual Connection in Kernel Space, respectively.

decay, dropout(different combinations for models with different model configurations), and stochastic depth [68] with a rate of 0.1. We also use Exponential Moving average (EMA) [69] with a momentum of 0.9995 for training.

Results of DMF. Table 2 shows the performances of the proposed DMFs that are specified in table 1. Our models consistently outperform efficient CNNs and multiple variants of vision transformers, with fewer FLOPs. In particular, our DMF-XXS achieves a 0.6% higher top-1 accuracy, while using only 60% of the FLOPs of MobileNetV2 [4] with ODConv(4x) [48]. This proves that our dynamic residual convolution with parallel design improves the representational power efficiently. We also compare our Dynamic Mobile-Former with various ViT variants(EdgeViT [54], Swin [29], BoT [61], CMT [38], MPViT [58]). Specifically, Compared to [29, 58], our DMFs achieve higher accuracy but use 3~4 times less computations. This is because that DMF uses efficient operators(group convolution [6], dynamic convolution [10]) combined with light-weight cross-attention with fewer tokens to extract local features effectively. Note that our DMF (trained in 470 epochs) even outperforms CMT-Tiny [38] which leverages much longer training (1000 epochs). We plot the accuracy-FLOPs curve in Fig. 1 (Left) to have an intuitive comparison between these methods. Prior works on dynamic convolution [9, 10, 47, 48] have shown efficiency, but their performance still falls short compared to low FLOPs regime efficient models. In contrast, our DMF maximizes representation power combining efficient operators and dynamic convolution in an appropriate manner, striking a balance between accuracy and FLOPs.

4.2. Object Detection and Instance Segmentation

Implementation Details. We validate our DMF as an efficient vision backbone for object detection and instance segmentation with RetinaNet [18] and Mask R-CNN [71], respectively. The experiments are conducted on COCO [17], which contains 118K training images and 5K validation images of 80 classes. We pretrain the backbones on the ImageNet-1K and replace the original backbones with our DMFs to generate multi-scale feature maps. For RetinaNet [18], All models are trained under standard single-scale and "1x" schedule (12 epochs) from ImageNet pre-

Backbone	#Params	FLOPs	mAP	AP ₅₀	AP ₇₅	AP _S	AP _M	AP _L
ShuffleNet-V2 [7]	10.4M	161G	25.9	41.9	26.9	12.4	28.0	36.4
MobileNet-V3 [5]	12.3M	162G	27.2	43.9	28.3	13.5	30.2	37.2
MobileFormer-151M [19]	14.4M	161G	34.2	53.4	36.0	19.9	36.8	45.3
DMF-XXS	17.4M	160G	35.3	54.8	37.0	19.1	37.9	47.6
ResNet50 [20]	38.0M	239G	36.3	55.3	38.6	19.3	40.4	48.8
MobileFormer-294M [19]	16.1M	164G	36.6	56.6	38.6	21.9	39.5	47.9
PVT-V2-B0 [70]	13.0M	177G	37.2	57.2	39.5	23.1	40.4	49.7
DMF-XS	20.2M	161G	37.3	57.2	39.8	21.4	40.1	50.1
ResNet101 [20]	56.7M	315G	38.5	57.6	41.0	21.7	42.8	50.4
PVT-V1-Tiny [30]	23.0M	221G	36.7	56.9	38.9	22.6	38.8	50.0
ConTNet-M [56]	27.0M	217G	37.9	58.1	40.2	23.0	40.6	50.4
MobileFormer-508M [19]	17.9M	168G	38.0	58.3	40.3	22.9	41.2	49.7
DMF-S	23.6M	165G	39.0	59.4	41.6	22.9	42.7	51.4

Table 4. **Object detection results on COCO val2017.** All models use RetinaNet [18] as basic framework and are trained on COCO [17] train2017 for 12 epochs (1 ×) with single-scale training inputs. All backbones are pretrained on ImageNet-1K. The FLOPs(G) are measured at resolution 800×1333.

Mask R-CNN 1×								
Backbone	#Params	FLOPs	AP ^b	AP ₅₀ ^b	AP ₇₅ ^b	AP ^m	AP ₅₀ ^m	AP ₇₅ ^m
ResNet50 [20]	44.0M	260G	38.0	58.6	41.4	34.4	55.1	36.7
PVT-V1-Tiny [30]	33.0M	240G	36.7	59.2	39.3	35.1	56.7	37.3
ResNet50 + DyConv [10] [‡]	121.8M	260G	39.2	60.3	42.5	-	-	-
PVT-V2-B0 [70]	23.0M	195G	38.2	60.5	40.7	36.2	57.8	38.6
DMF-S	34.2M	181G	39.8	61.6	43.0	37.1	58.8	39.8
Mask R-CNN 3×								
ResNet50 [20]	44.0M	260G	41.0	61.7	44.9	37.1	58.4	40.1
PVT-V1-Tiny [30]	33.0M	240G	39.8	62.2	43.0	37.4	59.3	39.9
DMF-S	34.2M	181G	42.4	63.9	46.3	39.0	61.2	41.7

Table 5. **Instance segmentation results on COCO val2017.** All models use Mask R-CNN [71] as basic framework and are trained on COCO [17] train2017 for 12 epochs (1 ×) with single-scale training inputs and 36 epochs(3 ×) with multi-scale training inputs. All backbones are pretrained on ImageNet-1K. The FLOPs(G) are measured at resolution 800×1333. [‡] means the results are from [48].

trained weights. For Mask R-CNN [71], we train models for both "1×" schedule and "3×" schedule (36 epochs) with a multi-scale training strategy [29]. We use AdamW [64] optimizer with an initial learning rate of 0.0001, weight decay of 0.0001, and a batch size of 16. We use the popular MMDetection toolbox [72] for experiments with all models.

Results of DMF. In Table 4 for object detection with RetinaNet, we compare our Dynamic Mobile-Former with efficient networks (CNNs : ShuffleNetV2 [7], MobileNetV3 [5], ResNet [20] ViTs : PVTs [30, 70], ConTNet [56] Hybrid : MobileFormer [19]). Under similar computational cost, our DMF surpasses ShuffleNetV2 [7], MobileNetV3 [5] by 9.4 points of mAP and 8.1 points of mAP respectively. Furthermore, it is worth noting that our DMF consistently outperforms MobileFormer [19] by a margin of 0.7 - 1.0% with less computations. For instance segmentation with Mask R-CNN, we report the performance comparison results of instance segmentation in Table 5. Our DMF-S achieves 42.4 AP^b, 39.0 AP^m, outperforming

ResNet50 [20] and PVT-Tiny [30] which consume more FLOPs (59 - 79G). This proves effectiveness of the proposed Dynamic Residual Convolution with light-weight attention features. See Fig. 1(Right) for intuitive comparison.

4.3. Ablations

In this section, we conduct ablation studies on each component of DMF-XXS to investigate the effectiveness of the proposed dynamic residual convolution on ImageNet classification.

Effectiveness of Dynamic residual convolution. As shown in Table 3, (a) inputting attention features to kernel attention module and (b) residual connection in kernel space only cost additional 4M FLOPs, but result in a 1.1% increase in top-1 accuracy over the baseline that use dynamic convolution [10]. While (a) alone has a relatively small impact on performance, it becomes more effective when used in combination with (b). It is worth noting that our proposed methods achieve meaningful improvements while incurring

activation	#Params	FLOPs	Top-1	Top-5
Softmax	15.1M	198.0M	72.8	90.6
Sigmoid	15.1M	198.0M	73.2	90.9

Table 6. **Ablation of activation in kernel attention module.** Here, DMF-XXS is used and all models are trained on ImageNet dataset for 150 epochs.

Init. method	#Params	FLOPs	Top-1	Top-5
Random	15.1M	198.0M	72.9	90.8
Zero	15.1M	198.0M	73.2	90.9

Table 7. **Ablation of initialization method for static kernel.** Here, DMF-XXS is used and all models are trained on ImageNet dataset for 150 epochs.

Kernel number	#Params	FLOPs	Top-1	Top-5
4	14.0M	196.8M	72.9	90.8
6	14.6M	197.4M	73.2	90.9
8	15.1M	198.0M	73.6	91.2

Table 8. **Ablation of static kernel number.** Here, DMF-XXS is used and all models are trained on ImageNet dataset for 150 epochs.

only negligible computational costs.

Activation function for attention scores. [9] proposed the use of sigmoid function to generate attention scores $\pi_k(x)$ in Eq.2. However incorporating sigmoid layer can result in a significantly large kernel space, which can make learning of the attention scores challenging. [10] stabilized the learning process by reducing the kernel space using softmax and demonstrated better performance with fewer kernels and FLOPs. But, as shown in the table 6, we utilize the sigmoid function to enhance performance by increasing the kernel space, as our residual connection in kernel space helps to alleviate optimization difficulties.

Initialization for W_{static} . We assume that the previous approach [9, 10] of using the dynamic convolution module to calculate both input-agnostic and input-dependent kernels in the kernel attention module results in optimization difficulties. Therefore, to address this issue, we introduce the residual connection that connects input-specific dynamic kernel to the existing input-agnostic kernel. The results presented in table 7 also align with the philosophy of the residual connection [20]. Note that input-agnostic kernel $W_{input_agnostic}$ is initialized randomly.

Static kernel number. We not only use temperature annealing to achieve stable training, but also utilize residual connection in kernel space to ease the optimization and expand the kernel space. Table 8 demonstrates that our dynamic residual convolution approach enables us to increase the kernel space by increasing the number of static kernels while maintaining stable training and improved performance.

Therefore, all variants of DMF take 8 static kernels, which is zero initialized and use sigmoid activation for generating attention scores.

5. Limitations

Our Dynamic Mobile-Former (DMF) has fewer FLOPs, but there are other factors that need to be considered for fast inference. For example, if memory access cost is high, then even if FLOPs are low, it may not be fast enough. In terms of memory access cost, the channel expansion in DY-Mobile and IRFFN is a bottleneck for DMF. For example, first point-wise convolution in DY-Mobile increase channels by 6 times, result in much higher memory access that can cause non-negligible delay and slow down the overall computations. Therefore, in future work, we will explore ways to reduce memory while actively utilizing our dynamic residual convolution. Additionally, our convolution module is computationally efficient but not parametrically efficient. Thus, exploring the application of omni-dimensional dynamic convolution [48] will also be an important research direction. Lastly, [73] introduce partial convolution more efficient than group convolution (depth-wise convolution) in terms of FLOPS(short for **f**loating-**p**oint **o**perations per second). We will investigate the combination of these newly proposed modules and our methods.

6. Conclusion

In this paper, we present a Dynamic Mobile-Former(DMF), a model that enhances the potential of dynamic convolution by combining it with efficient operators in a synergistic way. Our proposed dynamic residual convolution enhances stable learning by adding input-specific kernel to input-agnostic kernel. Based on this, we can further increase the model’s performance by actively expanding the kernel space. By integrating lightweight attention and enhanced dynamic convolution, our DMF achieves high efficiency and strong performance on a series of vision tasks. In particular, DMF demonstrates comparable performance to state-of-the-art models in image classification, and outperforms light-weight CNNs and vision transformer variants with significantly fewer FLOPs in object detection and instance segmentation. By simplifying the optimization process and effectively utilizing the capabilities of dynamic convolution, our DMF demonstrates the potential for further improvements in mobile vision applications.

References

- [1] Alexey Dosovitskiy, Lucas Beyer, Alexander Kolesnikov, Dirk Weissenborn, Xiaohua Zhai, Thomas Unterthiner, Mostafa Dehghani, Matthias Minderer, Georg Heigold, Sylvain Gelly, et al. An image is worth 16x16 words: Trans-

- formers for image recognition at scale. *arXiv preprint arXiv:2010.11929*, 2020. 1, 2, 3
- [2] Hugo Touvron, Matthieu Cord, Matthijs Douze, Francisco Massa, Alexandre Sablayrolles, and Hervé Jégou. Training data-efficient image transformers & distillation through attention. In *International conference on machine learning*, pages 10347–10357. PMLR, 2021. 1, 2
- [3] Andrew G Howard, Menglong Zhu, Bo Chen, Dmitry Kalenichenko, Weijun Wang, Tobias Weyand, Marco Andreetto, and Hartwig Adam. Mobilenets: Efficient convolutional neural networks for mobile vision applications. *arXiv preprint arXiv:1704.04861*, 2017. 1, 2
- [4] Mark Sandler, Andrew Howard, Menglong Zhu, Andrey Zhmoginov, and Liang-Chieh Chen. Mobilenetv2: Inverted residuals and linear bottlenecks. In *Proceedings of the IEEE conference on computer vision and pattern recognition*, pages 4510–4520, 2018. 1, 2, 3, 4, 6
- [5] Andrew Howard, Mark Sandler, Grace Chu, Liang-Chieh Chen, Bo Chen, Mingxing Tan, Weijun Wang, Yukun Zhu, Ruoming Pang, Vijay Vasudevan, et al. Searching for mobilenetv3. In *Proceedings of the IEEE/CVF international conference on computer vision*, pages 1314–1324, 2019. 1, 2, 5, 6, 7
- [6] Xiangyu Zhang, Xinyu Zhou, Mengxiao Lin, and Jian Sun. Shufflenet: An extremely efficient convolutional neural network for mobile devices. In *Proceedings of the IEEE conference on computer vision and pattern recognition*, pages 6848–6856, 2018. 1, 2, 6
- [7] Ningning Ma, Xiangyu Zhang, Hai-Tao Zheng, and Jian Sun. Shufflenet v2: Practical guidelines for efficient cnn architecture design. In *Proceedings of the European conference on computer vision (ECCV)*, pages 116–131, 2018. 1, 2, 7
- [8] Mingxing Tan and Quoc Le. Efficientnet: Rethinking model scaling for convolutional neural networks. In *International conference on machine learning*, pages 6105–6114. PMLR, 2019. 1, 2, 6
- [9] Brandon Yang, Gabriel Bender, Quoc V Le, and Jiquan Ngiam. Condcnv: Conditionally parameterized convolutions for efficient inference. *Advances in Neural Information Processing Systems*, 32, 2019. 1, 2, 3, 4, 6, 8
- [10] Yinpeng Chen, Xiyang Dai, Mengchen Liu, Dongdong Chen, Lu Yuan, and Zicheng Liu. Dynamic convolution: Attention over convolution kernels. In *Proceedings of the IEEE/CVF conference on computer vision and pattern recognition*, pages 11030–11039, 2020. 1, 2, 3, 4, 6, 7, 8
- [11] Jin Chen, Xijun Wang, Zichao Guo, Xiangyu Zhang, and Jian Sun. Dynamic region-aware convolution. In *Proceedings of the IEEE/CVF Conference on Computer Vision and Pattern Recognition*, pages 8064–8073, 2021. 1
- [12] Ningning Ma, Xiangyu Zhang, Jiawei Huang, and Jian Sun. Weightnet: Revisiting the design space of weight networks. In *Computer Vision–ECCV 2020: 16th European Conference, Glasgow, UK, August 23–28, 2020, Proceedings, Part XV*, pages 776–792. Springer, 2020. 1
- [13] Zhi Tian, Chunhua Shen, and Hao Chen. Conditional convolutions for instance segmentation. In *Computer Vision–ECCV 2020: 16th European Conference, Glasgow, UK, August 23–28, 2020, Proceedings, Part I 16*, pages 282–298. Springer, 2020. 1
- [14] Tong He, Chunhua Shen, and Anton Van Den Hengel. Dyc3d: Robust instance segmentation of 3d point clouds through dynamic convolution. In *Proceedings of the IEEE/CVF conference on computer vision and pattern recognition*, pages 354–363, 2021. 1
- [15] Jie Liu, Yanqi Bao, Guo-Sen Xie, Huan Xiong, Jan-Jakob Sonke, and Efstratios Gavves. Dynamic prototype convolution network for few-shot semantic segmentation. In *Proceedings of the IEEE/CVF Conference on Computer Vision and Pattern Recognition*, pages 11553–11562, 2022. 1
- [16] Jia Deng, Wei Dong, Richard Socher, Li-Jia Li, Kai Li, and Li Fei-Fei. Imagenet: A large-scale hierarchical image database. In *2009 IEEE conference on computer vision and pattern recognition*, pages 248–255. Ieee, 2009. 2, 6
- [17] Tsung-Yi Lin, Michael Maire, Serge Belongie, James Hays, Pietro Perona, Deva Ramanan, Piotr Dollár, and C Lawrence Zitnick. Microsoft coco: Common objects in context. In *Computer Vision–ECCV 2014: 13th European Conference, Zurich, Switzerland, September 6–12, 2014, Proceedings, Part V 13*, pages 740–755. Springer, 2014. 2, 6, 7
- [18] Tsung-Yi Lin, Priya Goyal, Ross Girshick, Kaiming He, and Piotr Dollár. Focal loss for dense object detection. In *Proceedings of the IEEE international conference on computer vision*, pages 2980–2988, 2017. 2, 6, 7
- [19] Yinpeng Chen, Xiyang Dai, Dongdong Chen, Mengchen Liu, Xiaoyi Dong, Lu Yuan, and Zicheng Liu. Mobileformer: Bridging mobilenet and transformer. In *Proceedings of the IEEE/CVF Conference on Computer Vision and Pattern Recognition*, pages 5270–5279, 2022. 2, 3, 5, 6, 7
- [20] Kaiming He, Xiangyu Zhang, Shaoqing Ren, and Jian Sun. Deep residual learning for image recognition. In *Proceedings of the IEEE conference on computer vision and pattern recognition*, pages 770–778, 2016. 2, 6, 7, 8
- [21] Mingxing Tan, Ruoming Pang, and Quoc V Le. Efficientdet: Scalable and efficient object detection. In *Proceedings of the IEEE/CVF conference on computer vision and pattern recognition*, pages 10781–10790, 2020. 2
- [22] Kai Han, Yunhe Wang, Qi Tian, Jianyuan Guo, Chunjing Xu, and Chang Xu. Ghostnet: More features from cheap operations. In *Proceedings of the IEEE/CVF conference on computer vision and pattern recognition*, pages 1580–1589, 2020. 2
- [23] Mingxing Tan and Quoc V Le. Mixconv: Mixed depthwise convolutional kernels. *arXiv preprint arXiv:1907.09595*, 2019. 2
- [24] Hanqing Chen, Yunhe Wang, Chunjing Xu, Boxin Shi, Chao Xu, Qi Tian, and Chang Xu. Addernet: Do we really need multiplications in deep learning? In *Proceedings of the IEEE/CVF Conference on Computer Vision and Pattern Recognition (CVPR)*, June 2020. 2

- [25] Ashish Vaswani, Noam Shazeer, Niki Parmar, Jakob Uszkoreit, Llion Jones, Aidan N Gomez, Łukasz Kaiser, and Illia Polosukhin. Attention is all you need. *Advances in neural information processing systems*, 30, 2017. 2, 4
- [26] Xiangxiang Chu, Zhi Tian, Bo Zhang, Xinlong Wang, Xiaolin Wei, Huaxia Xia, and Chunhua Shen. Conditional positional encodings for vision transformers. *arXiv preprint arXiv:2102.10882*, 2021. 2
- [27] Kai Han, An Xiao, Enhua Wu, Jianyuan Guo, Chunjing Xu, and Yunhe Wang. Transformer in transformer. *Advances in Neural Information Processing Systems*, 34:15908–15919, 2021. 2
- [28] Wenshuo Li, Hanting Chen, Jianyuan Guo, Ziyang Zhang, and Yunhe Wang. Brain-inspired multilayer perceptron with spiking neurons. In *Proceedings of the IEEE/CVF Conference on Computer Vision and Pattern Recognition*, pages 783–793, 2022. 2
- [29] Ze Liu, Yutong Lin, Yue Cao, Han Hu, Yixuan Wei, Zheng Zhang, Stephen Lin, and Baining Guo. Swin transformer: Hierarchical vision transformer using shifted windows. In *Proceedings of the IEEE/CVF international conference on computer vision*, pages 10012–10022, 2021. 2, 6, 7
- [30] Wenhai Wang, Enze Xie, Xiang Li, Deng-Ping Fan, Kaitao Song, Ding Liang, Tong Lu, Ping Luo, and Ling Shao. Pyramid vision transformer: A versatile backbone for dense prediction without convolutions. In *Proceedings of the IEEE/CVF international conference on computer vision*, pages 568–578, 2021. 2, 6, 7
- [31] Haiping Wu, Bin Xiao, Noel Codella, Mengchen Liu, Xiyang Dai, Lu Yuan, and Lei Zhang. Cvt: Introducing convolutions to vision transformers. In *Proceedings of the IEEE/CVF International Conference on Computer Vision*, pages 22–31, 2021. 2
- [32] Nicolas Carion, Francisco Massa, Gabriel Synnaeve, Nicolas Usunier, Alexander Kirillov, and Sergey Zagoruyko. End-to-end object detection with transformers. In *Computer Vision—ECCV 2020: 16th European Conference, Glasgow, UK, August 23–28, 2020, Proceedings, Part I 16*, pages 213–229. Springer, 2020. 2
- [33] Xizhou Zhu, Weijie Su, Lewei Lu, Bin Li, Xiaogang Wang, and Jifeng Dai. Deformable detr: Deformable transformers for end-to-end object detection. *arXiv preprint arXiv:2010.04159*, 2020. 2
- [34] Ishan Misra, Rohit Girdhar, and Armand Joulin. An end-to-end transformer model for 3d object detection. In *Proceedings of the IEEE/CVF International Conference on Computer Vision*, pages 2906–2917, 2021. 2
- [35] Enze Xie, Wenhai Wang, Zhiding Yu, Anima Anandkumar, Jose M Alvarez, and Ping Luo. Segformer: Simple and efficient design for semantic segmentation with transformers. *Advances in Neural Information Processing Systems*, 34:12077–12090, 2021. 2
- [36] Namuk Park and Songkuk Kim. How do vision transformers work? *arXiv preprint arXiv:2202.06709*, 2022. 2, 3
- [37] Chenyang Si, Weihao Yu, Pan Zhou, Yichen Zhou, Xinchao Wang, and Shuicheng Yan. Inception transformer. *arXiv preprint arXiv:2205.12956*, 2022. 2
- [38] Jianyuan Guo, Kai Han, Han Wu, Yehui Tang, Xinghao Chen, Yunhe Wang, and Chang Xu. Cmt: Convolutional neural networks meet vision transformers. In *Proceedings of the IEEE/CVF Conference on Computer Vision and Pattern Recognition*, pages 12175–12185, 2022. 2, 4, 5, 6
- [39] Tete Xiao, Mannat Singh, Eric Mintun, Trevor Darrell, Piotr Dollár, and Ross Girshick. Early convolutions help transformers see better. *Advances in Neural Information Processing Systems*, 34:30392–30400, 2021. 2
- [40] Zihang Dai, Hanxiao Liu, Quoc V Le, and Mingxing Tan. Coatnet: Marrying convolution and attention for all data sizes. *Advances in Neural Information Processing Systems*, 34:3965–3977, 2021. 2
- [41] Weijian Xu, Yifan Xu, Tyler Chang, and Zhuowen Tu. Co-scale conv-attentional image transformers. In *Proceedings of the IEEE/CVF International Conference on Computer Vision*, pages 9981–9990, 2021. 2
- [42] Yufei Xu, Qiming Zhang, Jing Zhang, and Dacheng Tao. Vitae: Vision transformer advanced by exploring intrinsic inductive bias. *Advances in Neural Information Processing Systems*, 34:28522–28535, 2021. 2, 3
- [43] Andrew Jaegle, Felix Gimeno, Andy Brock, Oriol Vinyals, Andrew Zisserman, and Joao Carreira. Perceiver: General perception with iterative attention. In *International conference on machine learning*, pages 4651–4664. PMLR, 2021. 3
- [44] Yinpeng Chen, Xiyang Dai, Mengchen Liu, Dongdong Chen, Lu Yuan, and Zicheng Liu. Dynamic relu. In *Computer Vision—ECCV 2020: 16th European Conference, Glasgow, UK, August 23–28, 2020, Proceedings, Part XIX 16*, pages 351–367. Springer, 2020. 3
- [45] Jie Hu, Li Shen, and Gang Sun. Squeeze-and-excitation networks. In *Proceedings of the IEEE conference on computer vision and pattern recognition*, pages 7132–7141, 2018. 3
- [46] Sanghyun Woo, Jongchan Park, Joon-Young Lee, and In So Kweon. Cbam: Convolutional block attention module. In *Proceedings of the European conference on computer vision (ECCV)*, pages 3–19, 2018. 3
- [47] Yunsheng Li, Yinpeng Chen, Xiyang Dai, Mengchen Liu, Dongdong Chen, Ye Yu, Lu Yuan, Zicheng Liu, Mei Chen, and Nuno Vasconcelos. Revisiting dynamic convolution via matrix decomposition. *arXiv preprint arXiv:2103.08756*, 2021. 3, 6
- [48] Chao Li, Aojun Zhou, and Anbang Yao. Omni-dimensional dynamic convolution. *arXiv preprint arXiv:2209.07947*, 2022. 3, 6, 7, 8
- [49] Dan Hendrycks and Kevin Gimpel. Gaussian error linear units (gelus). *arXiv preprint arXiv:1606.08415*, 2016. 4, 5
- [50] Zhuang Liu, Hanzi Mao, Chao-Yuan Wu, Christoph Feichtenhofer, Trevor Darrell, and Saining Xie. A convnet for the

- 2020s. In *Proceedings of the IEEE/CVF Conference on Computer Vision and Pattern Recognition*, pages 11976–11986, 2022. 4
- [51] Yunsheng Li, Yinpeng Chen, Xiyang Dai, Dongdong Chen, Mengchen Liu, Lu Yuan, Zicheng Liu, Lei Zhang, and Nuno Vasconcelos. Micronet: Towards image recognition with extremely low flops. *arXiv preprint arXiv:2011.12289*, 2020. 5
- [52] Sergey Ioffe and Christian Szegedy. Batch normalization: Accelerating deep network training by reducing internal covariate shift. In *International conference on machine learning*, pages 448–456. pmlr, 2015. 5
- [53] Sanghyun Woo, Shoubhik Debnath, Ronghang Hu, Xinlei Chen, Zhuang Liu, In So Kweon, and Saining Xie. Convnext v2: Co-designing and scaling convnets with masked autoencoders. *arXiv preprint arXiv:2301.00808*, 2023. 5
- [54] Junting Pan, Adrian Bulat, Fuwen Tan, Xiatian Zhu, Lukasz Dudziak, Hongsheng Li, Georgios Tzimiropoulos, and Brais Martinez. Edgevits: Competing light-weight cnns on mobile devices with vision transformers. In *Computer Vision–ECCV 2022: 17th European Conference, Tel Aviv, Israel, October 23–27, 2022, Proceedings, Part XI*, pages 294–311. Springer, 2022. 6
- [55] Muhammad Maaz, Abdelrahman Shaker, Hisham Cholakkal, Salman Khan, Syed Waqas Zamir, Rao Muhammad Anwer, and Fahad Shahbaz Khan. Edgenext: efficiently amalgamated cnn-transformer architecture for mobile vision applications. In *Computer Vision–ECCV 2022 Workshops: Tel Aviv, Israel, October 23–27, 2022, Proceedings, Part VII*, pages 3–20. Springer, 2023. 6
- [56] Haotian Yan, Zhe Li, Weijian Li, Changhu Wang, Ming Wu, and Chuang Zhang. Contnet: Why not use convolution and transformer at the same time? *arXiv preprint arXiv:2104.13497*, 2021. 6, 7
- [57] Han Cai, Chuang Gan, and Song Han. Efficientvit: Enhanced linear attention for high-resolution low-computation visual recognition. *arXiv preprint arXiv:2205.14756*, 2022. 6
- [58] Youngwan Lee, Jonghee Kim, Jeffrey Willette, and Sung Ju Hwang. Mpvit: Multi-path vision transformer for dense prediction. In *Proceedings of the IEEE/CVF Conference on Computer Vision and Pattern Recognition*, pages 7287–7296, 2022. 6
- [59] Sachin Mehta and Mohammad Rastegari. Mobilevit: light-weight, general-purpose, and mobile-friendly vision transformer. *arXiv preprint arXiv:2110.02178*, 2021. 6
- [60] Mingxing Tan and Quoc Le. Efficientnetv2: Smaller models and faster training. In *International conference on machine learning*, pages 10096–10106. PMLR, 2021. 6
- [61] Aravind Srinivas, Tsung-Yi Lin, Niki Parmar, Jonathon Shlens, Pieter Abbeel, and Ashish Vaswani. Bottleneck transformers for visual recognition. In *Proceedings of the IEEE/CVF conference on computer vision and pattern recognition*, pages 16519–16529, 2021. 6
- [62] Adam Paszke, Sam Gross, Francisco Massa, Adam Lerer, James Bradbury, Gregory Chanan, Trevor Killeen, Zeming Lin, Natalia Gimelshein, Luca Antiga, et al. Pytorch: An imperative style, high-performance deep learning library. *Advances in neural information processing systems*, 32, 2019. 6
- [63] Ross Wightman. Pytorch image models. <https://github.com/rwightman/pytorch-image-models>, 2019. 6
- [64] Ilya Loshchilov and Frank Hutter. Decoupled weight decay regularization. *arXiv preprint arXiv:1711.05101*, 2017. 6, 7
- [65] Ilya Loshchilov and Frank Hutter. Sgdr: Stochastic gradient descent with warm restarts. *arXiv preprint arXiv:1608.03983*, 2016. 6
- [66] Zhun Zhong, Liang Zheng, Guoliang Kang, Shaozi Li, and Yi Yang. Random erasing data augmentation. In *Proceedings of the AAAI conference on artificial intelligence*, volume 34, pages 13001–13008, 2020. 6
- [67] Ekin D Cubuk, Barret Zoph, Jonathon Shlens, and Quoc V Le. Randaugment: Practical automated data augmentation with a reduced search space. In *Proceedings of the IEEE/CVF conference on computer vision and pattern recognition workshops*, pages 702–703, 2020. 6
- [68] Gao Huang, Yu Sun, Zhuang Liu, Daniel Sedra, and Kilian Q Weinberger. Deep networks with stochastic depth. In *Computer Vision–ECCV 2016: 14th European Conference, Amsterdam, The Netherlands, October 11–14, 2016, Proceedings, Part IV 14*, pages 646–661. Springer, 2016. 6
- [69] Boris T Polyak and Anatoli B Juditsky. Acceleration of stochastic approximation by averaging. *SIAM journal on control and optimization*, 30(4):838–855, 1992. 6
- [70] Wenhai Wang, Enze Xie, Xiang Li, Deng-Ping Fan, Kaitao Song, Ding Liang, Tong Lu, Ping Luo, and Ling Shao. Pvt v2: Improved baselines with pyramid vision transformer. *Computational Visual Media*, 8(3):415–424, 2022. 7
- [71] Kaiming He, Georgia Gkioxari, Piotr Dollár, and Ross Girshick. Mask r-cnn. In *Proceedings of the IEEE international conference on computer vision*, pages 2961–2969, 2017. 6, 7
- [72] Kai Chen, Jiaqi Wang, Jiangmiao Pang, Yuhang Cao, Yu Xiong, Xiaoxiao Li, Shuyang Sun, Wansen Feng, Ziwei Liu, Jiarui Xu, Zheng Zhang, Dazhi Cheng, Chenchen Zhu, Tianheng Cheng, Qijie Zhao, Buyu Li, Xin Lu, Rui Zhu, Yue Wu, Jifeng Dai, Jingdong Wang, Jianping Shi, Wanli Ouyang, Chen Change Loy, and Dahua Lin. MMDetection: Open mmlab detection toolbox and benchmark. *arXiv preprint arXiv:1906.07155*, 2019. 7
- [73] Jierun Chen, Shiu-hong Kao, Hao He, Weipeng Zhuo, Song Wen, Chul-Ho Lee, and S-H Gary Chan. Run, don’t walk: Chasing higher flops for faster neural networks. *arXiv preprint arXiv:2303.03667*, 2023. 8